

Maneuvering Target Tracking Using Current Statistical Model Based Adaptive UKF for Wireless Sensor Network

Xiaojun Peng^{1,2}, Kuntao Yang¹, and Chang Liu²

¹School of Optical and Electronic Information, Huazhong University of Science and Technology, Wuhan, 430074, China

²Wuhan Second Ship Design Research Institute, Wuhan, 430064, China
Email: {kingarthurpeng, imliuchang}@hotmail.com; yangkuntao@mail.hust.edu.cn

Abstract—This paper presents Current statistical model based Adaptive Unscented Kalman Filter (CAUKF) for maneuvering target tracking, which is based on Received Signal Strength Indication (RSSI). In order to introduce the Kalman filter, the state-space model, which uses RSSI values as the measurement equation, needs to be obtained. Thus a current statistical model for maneuvering target based on the path loss model is presented. To avoid the negative influence of current statistical model's limited acceleration, the functional relation between the maneuvering status of target and the estimation of the neighboring position information is applied to carry out the adaptation of the process noise covariance $Q(k)$. Then, a novel idea of modified Sage-Husa estimator is introduced to adapt the process noise covariance matrix $Q(k)$, while the adaptive measurement noise covariance matrix $R(k)$ is implemented by a fuzzy inference system. The experimental results show that the final improved CAUKF is an algorithm with faster response and better tracking accuracy especially in maneuvering target tracking.

Index Terms—Maneuvering target tracking, adaptive unscented kalman filter, current statistical model, wireless sensor network, received signal strength indication

I. INTRODUCTION

The development pace of target tracking research is highly tied up with the advancement of Wireless Sensor Network (WSN) and wireless technologies. As sensor nodes in WSN become smaller and stronger, the ability of information processing is much stronger and wireless network operation management is also more intelligent. At present, many target tracking algorithms for wireless system have been proposed. Because Radio Frequency Identification (RFID) based tracking technology is low-cost and operable, so it is used widely in practical applications. The particular interest is the ability to track targets carrying active RFID tags, by exploiting metrics of their periodic transmissions such as Time of Arrival (TOA), Time Difference of Arrival (TDOA), Angle of Arrival (AOA), and Received Signal Strength Indication (RSSI) [1]. The traditional RSSI based tracking method

that is called triangulation method always uses a set of reference nodes to locate an unknown node, which converts the RSSI values from each reference node into distance estimate [2], [3]. The triangulation method relies on the measurements from each reference node, which has the intersection area. However, the distance estimates do not always intersect due to noise interference, making it virtually impossible to triangulate the position of the unknown node. Hence a recursive method capable of maintaining a position estimate must be used to guarantee state estimates even when no RSSI measurements are available or they are highly corrupted by noise.

State-space model is a powerful tracking technique that relies on a maneuvering model for the estimate of the unknown node position and an observation model that relates the position to observed measurements between the reference nodes and the unknown node [4]. If the model is linear, the classical Kalman filter [5] is optimal for the state estimation. Unfortunately, this is a rare occurrence in practice because measurement model based on path loss model is nonlinear. A common approach to overcome this problem is to linearize the system before using the Kalman filter, resulting in the Extended Kalman Filter (EKF) [6]. EKF is the most widely used filtering method for nonlinear dynamic system. However, this method of linearization may introduce large errors in a posteriori mean and covariance of the state estimation. In light of the intuition that to approximate a probability distribution is easier than to approximate an arbitrary nonlinear transformation, a novel filter called Unscented Kalman Filter (UKF) [7] was presented. In particular, the UKF matches the mean correctly up to the second order in Taylor series and predicts the covariance correctly up to the third order, while the EKF can only approximate the mean up to the first order. However, like classical Kalman filter, the traditional UKF formulation assumes complete a priori knowledge of the process noise covariance matrix $Q(k)$ and the measurement noise covariance matrix $R(k)$. In most practical applications, these matrices are initially estimated or, in fact, are unknown. The problem here is that the optimality of the estimation algorithm in the UKF setting is closely connected to the quality of these a priori noise matrices. Calculation of the matrices $Q(k)$ and $R(k)$ for a particular measurement system is a straight-forward process, but it

Manuscript received May 2, 2015; revised July 27, 2015.

This work was supported by the National Natural Science Foundation of China under Grant No. 61275081.

Corresponding author email: kingarthurpeng@hotmail.com.

doi:10.12720/jcm.10.8.579-588.

is not guaranteed that $Q(k)$ and $R(k)$ remain constant with time going by in highly non-stationary noise conditions, so it is imperative to continuously tune the UKF in view of the changing noise conditions in order to get good filtering performance.

In this paper, a novel fuzzy adaptive UKF is introduced. Based on the current statistical model [8], a developed adaptive UKF algorithm is proposed, which estimates the process noise covariance matrix $Q(k)$ by a new formula. Then an improved fuzzy adaptive UKF is applied to estimate the covariance matrix $R(k)$. The experimental results show that the final improved adaptive UKF can reduce prediction error and sense the variation of motion faster. It is compared with the conventional Current statistical model based UKF (CUKF) [9], the traditional Current statistical model based Adaptive Unscented Kalman Filter (CAUKF) and the Adaptive UKF (AUKF) using method in [10].

The remainder of the paper is organized as follows. In Section II, an adaptive current statistical model based UKF is introduced. In Section III, an improved adaptive

UKF is presented. Section IV describes simulation results of the algorithms. Numerical experiment results are provided in Section V. Finally, Section VI provides the conclusion for this paper.

II. CURRENT STATISTICAL MODEL BASED UKF

Current statistical model is a kind of time-correlated model with non-zero mean. It is assumed that the acceleration of target $\alpha(t)$ [9], [11] is defined by

$$a(t) = \hat{a}(t) + \bar{a}(t) \tag{1}$$

where $\hat{a}(t)$ is zero-mean Markov process, $\bar{a}(t)$ is the mean of acceleration, assumed to be constant in every sampling period. The current statistical model [9], [11] based on RSSI is denoted as

$$\begin{aligned} X(k) &= \Phi(k)X(k-1) + U(k)\bar{a} + W(k) \\ RSSI(k) &= f(X(k)) + V(k) \end{aligned} \tag{2}$$

with

$$\Phi(k) = \begin{pmatrix} 1 & T & \frac{1}{\alpha^2}(\alpha T - 1 + e^{-\alpha T}) & 0 & 0 & 0 & 0 & 0 & 0 \\ 0 & 1 & \frac{1}{\alpha}(1 - e^{-\alpha T}) & 0 & 0 & 0 & 0 & 0 & 0 \\ 0 & 0 & e^{-\alpha T} & 0 & 0 & 0 & 0 & 0 & 0 \\ 0 & 0 & 0 & 1 & T & \frac{1}{\alpha^2}(\alpha T - 1 + e^{-\alpha T}) & 0 & 0 & 0 \\ 0 & 0 & 0 & 0 & 1 & \frac{1}{\alpha}(1 - e^{-\alpha T}) & 0 & 0 & 0 \\ 0 & 0 & 0 & 0 & 0 & e^{-\alpha T} & 0 & 0 & 0 \\ 0 & 0 & 0 & 0 & 0 & 0 & 1 & T & \frac{1}{\alpha^2}(\alpha T - 1 + e^{-\alpha T}) \\ 0 & 0 & 0 & 0 & 0 & 0 & 0 & 1 & \frac{1}{\alpha}(1 - e^{-\alpha T}) \\ 0 & 0 & 0 & 0 & 0 & 0 & 0 & 0 & e^{-\alpha T} \end{pmatrix} \tag{3}$$

$$U(k) = \begin{pmatrix} \frac{1}{\alpha}(\frac{\alpha T^2}{2} + \frac{1 - e^{-\alpha T}}{\alpha} - T) & 0 & 0 \\ T - \frac{1 - e^{-\alpha T}}{\alpha} & 0 & 0 \\ 1 - e^{-\alpha T} & 0 & 0 \\ 0 & \frac{1}{\alpha}(\frac{\alpha T^2}{2} + \frac{1 - e^{-\alpha T}}{\alpha} - T) & 0 \\ 0 & T - \frac{1 - e^{-\alpha T}}{\alpha} & 0 \\ 0 & 1 - e^{-\alpha T} & 0 \\ 0 & 0 & \frac{1}{\alpha}(\frac{\alpha T^2}{2} + \frac{1 - e^{-\alpha T}}{\alpha} - T) \\ 0 & 0 & T - \frac{1 - e^{-\alpha T}}{\alpha} \\ 0 & 0 & 1 - e^{-\alpha T} \end{pmatrix} \tag{4}$$

where $X(k)=[x \ \dot{x} \ \ddot{x} \ y \ \dot{y} \ \ddot{y} \ z \ \dot{z} \ \ddot{z}]$. x, y and z are the predicted coordinates of the maneuvering target in three dimensional space, the predicted velocities of the target in three dimensional coordinate system are represented by \dot{x}, \dot{y} and \dot{z} respectively, \ddot{x}, \ddot{y} and \ddot{z} are the predicted accelerations of the maneuvering target, while $RSSI(k)=[RSSI_1 \ RSSI_2 \ RSSI_3 \ RSSI_4]$ is the RSSI vector, which is made up of the RSSI values between the unknown node and reference nodes. α is acceleration correlation coefficient. $V(k)$ is zero-mean white Gaussian noise, whose variance is $R(k)$. The process noise $W(k)$ is a discrete time sequence of white noise, and $E[W(k)W^T(k+j)]=0, (\forall j \neq 0)$. Process noise covariance matrix is given by

$$Q(k) = E[W(k)W^T(k)] = 2\alpha\sigma_a^2 \begin{pmatrix} q_{11} & q_{12} & q_{13} \\ q_{12} & q_{22} & q_{23} \\ q_{13} & q_{23} & q_{33} \end{pmatrix} \quad (5)$$

where

$$\begin{aligned} q_{11} &= \frac{1}{2\alpha^5} \left(1 - e^{-2\alpha T} + 2\alpha T + \frac{2\alpha^3 T^3}{3} - 2\alpha^2 T^2 - 4\alpha T e^{-\alpha T} \right) \\ q_{12} &= \frac{1}{2\alpha^4} \left(e^{-2\alpha T} + 1 + 2e^{-\alpha T} + 2\alpha T e^{-\alpha T} - 2\alpha T - \alpha^2 T^2 \right) \\ q_{13} &= \frac{1}{2\alpha^3} (1 - e^{-2\alpha T} - 2\alpha T e^{-\alpha T}) \\ q_{22} &= \frac{1}{2\alpha^3} (4e^{-\alpha T} - 3 - e^{-2\alpha T} + 2\alpha T) \\ q_{23} &= \frac{1}{2\alpha^2} (e^{-2\alpha T} + 1 - 2e^{-\alpha T}) \\ q_{33} &= \frac{1}{2\alpha} (1 - e^{-2\alpha T}) \end{aligned} \quad (6)$$

σ_a^2 is the modified Rayleigh distribution variance of the maneuvering acceleration as shown in (7),

$$\begin{cases} \sigma_a^2 = \frac{4-\pi}{\pi} [a_{\max} - \hat{a}(t)]^2, & \hat{a}(t) > 0 \\ \sigma_a^2 = \frac{4-\pi}{\pi} [-a_{\max} + \hat{a}(t)]^2, & \hat{a}(t) < 0 \end{cases} \quad (7)$$

where a_{\max} is the positive upper limit of the acceleration, while a_{\min} is the negative lower limit of the acceleration, $\hat{a}(t)$ is the current predicted acceleration. In this paper, state-space model based on RSSI is improved and extended to three-dimensional space. In two-dimensional space, three reference nodes are required at least to locate one unknown node. However, four nodes are needed at least in three-dimensional space. Hence four given nodes $A(x_1, y_1, z_1), B(x_2, y_2, z_2), C(x_3, y_3, z_3), D(x_4, y_4, z_4)$ are chosen, the RSSI values between the unknown moving node and the four reference nodes are measured. The measurement equation, which is based on path loss model [12], corresponding to RSSI is given by

$$RSSI_i = RSSI(1m) - 10\eta \lg \sqrt{(x-x_i)^2 + (y-y_i)^2 + (z-z_i)^2} \quad (8)$$

$i = 1, 2, 3, 4$

Assume the nonlinear system is given by (1) and (2), the standard UKF [6] algorithm can be summarized as follows.

Given the state vector at timestep $k-1$, a set of sigma points are generated and stored in columns of the $N \times (2N+1)$ sigma point matrix χ_{k-1} , where N is the dimension of the state vector. The sigma points are selected to lie on the principal component axes of the covariance $P(k-1|k-1)$, and include an extra point $\bar{X}(k-1)$. The sigma points are computed by

$$\chi_{0,k-1} = \bar{X}(k-1) \quad (9)$$

$$\chi_{i,k-1} = \bar{X}(k-1) + (\sqrt{(N+\gamma)P(k-1)})_i, \quad i = 1, \dots, N \quad (10)$$

$$\begin{aligned} \chi_{i,k-1} &= \bar{X}(k-1) - (\sqrt{(N+\gamma)P(k-1)})_{i-N} \\ & \quad i = N+1, \dots, 2N \end{aligned} \quad (11)$$

where γ is a scale parameter that determines how far the sigma points are spread from the mean and is defined by

$$\gamma = \alpha^2 (N + \kappa) - N \quad (12)$$

where α determines the spread of the sigma points around $\bar{X}(k-1)$ and is usually set to a small positive value (e.g. $10^{-4} \leq \alpha \leq 1$), and κ is a secondary scale parameter that approximates the higher-order terms and is usually set to either 0 or $3-N$. The prediction step or time update is performed by propagating the generated sigma points through the state equation. The propagated sigma points are then combined with associated weights to produce the predicted state and covariance.

The time update equations are

$$X_i^*(k|k-1) = \Phi(k)\chi_{i,k-1} + U(k)\bar{a}(k-1|k-1) \quad (13)$$

$$X(k|k-1) = \sum_{i=0}^{2N} W_i^{(m)} X_i^*(k|k-1) \quad (14)$$

$$\begin{aligned} P(k|k-1) &= \sum_{i=0}^{2N} W_i^{(c)} \left([X_i^*(k|k-1) - X(k|k-1)] \times \right. \\ & \quad \left. [X_i^*(k|k-1) - X(k|k-1)]^T \right) + Q(k-1) \end{aligned} \quad (15)$$

where $W_i^{(m)}$ and $W_i^{(c)}$ are the weights defined by

$$W_0^{(m)} = \frac{\kappa}{N + \kappa}, \quad W_0^{(c)} = \frac{\kappa}{N + \kappa} + (1 - \alpha^2 + \beta),$$

$$W_i^{(c)} = W_i^{(m)} = \frac{1}{2(N + \kappa)}, \quad i = 1, \dots, 2N \quad (16)$$

where β is used to incorporate a priori knowledge of the distribution of X and for a Gaussian distribution, $\beta = 2$ is optimal.

To compute the measurement update, the sigma points are transformed through the nonlinear measurement equation to obtain the predicted RSSI estimates using

$$RSSI_i^*(k|k-1) = f(X_i^*(k|k-1)) \quad (17)$$

$$RSSI(k|k-1) = \sum_{i=0}^{2N} W_i^{(m)} RSSI_i^*(k|k-1) \quad (18)$$

With the transformed state vector $RSSI(k|k-1)$, a posteriori state estimate is computed using

$$X(k|k) = X(k|k-1) + K(k) \times [RSSI(k) - RSSI(k|k-1)] \quad (19)$$

where $K(k)$ is the Kalman filter gain and defined by

$$K(k) = P_{xz} P_{zz}^{-1} \quad (20)$$

$$P_{zz} = \sum_{i=0}^{2N} W_i^{(m)} ([RSSI_i^*(k|k-1) - RSSI(k|k-1)] \times [RSSI_i^*(k|k-1) - RSSI(k|k-1)]^T) + R \quad (21)$$

$$P_{xz} = \sum_{i=0}^{2N} W_i^{(m)} ([X_i^*(k|k-1) - X(k|k-1)] \times [RSSI_i^*(k|k-1) - RSSI(k|k-1)]^T) \quad (22)$$

Two significant covariance matrices, P_{zz} and P_{xz} are used here. During the iterative process P_{zz} will be reduced so that the transformed sigma points move towards the cluster mean. With the introduction of the measurement data $RSSI(k)$, the cluster mean will then move further towards the true mean. As a result, P_{xz} will be reduced. R is the measurement noise covariance matrix. Finally, a posteriori estimate of the error covariance is given by

$$P(k|k) = P(k|k-1) - K(k) P_{zz} K^T(k) \quad (23)$$

$a(k-1|k-1) = [\ddot{x}(k-1|k-1) \quad \ddot{y}(k-1|k-1) \quad \ddot{z}(k-1|k-1)]^T$ is the prediction of $[\ddot{x}(k) \quad \ddot{y}(k) \quad \ddot{z}(k)]^T$ and regarded as \bar{a} (i.e., the mean of accelerations) here. Then (13) can be rewritten as

$$\begin{cases} X_i^*(k|k-1) = \Phi(k) \chi_{i,k-1} + U(k) \bar{a}(k-1|k-1) = \\ \Phi'(k) \chi_{i,k-1} + \Phi(k) \sqrt{(N+\gamma)P(k-1)}_i \quad i = 1, \dots, N \\ \Phi'(k) \chi_{i,k-1} - \Phi(k) \sqrt{(N+\gamma)P(k-1)}_{i-N} \quad i = N+1, \dots, 2N \end{cases} \quad (24)$$

where

$$\Phi'(k) = \begin{pmatrix} 1 & T & \frac{T^2}{2} & 0 & 0 & 0 & 0 & 0 & 0 \\ 0 & 1 & T & 0 & 0 & 0 & 0 & 0 & 0 \\ 0 & 0 & 1 & 0 & 0 & 0 & 0 & 0 & 0 \\ 0 & 0 & 0 & 1 & T & \frac{T^2}{2} & 0 & 0 & 0 \\ 0 & 0 & 0 & 0 & 1 & T & 0 & 0 & 0 \\ 0 & 0 & 0 & 0 & 0 & 1 & 0 & 0 & 0 \\ 0 & 0 & 0 & 0 & 0 & 0 & 1 & T & \frac{T^2}{2} \\ 0 & 0 & 0 & 0 & 0 & 0 & 0 & 1 & T \\ 0 & 0 & 0 & 0 & 0 & 0 & 0 & 0 & 1 \end{pmatrix}$$

Hence the unscented Kalman algorithm is fulfilled.

III. IMPROVED ADAPTIVE UKF

A. Adaptive Algorithm of Process Noise Covariance Matrix $Q(k)$

The algorithm mentioned above is affected by a_{\max} and $a_{-\max}$ greatly. If the absolute values of a_{\max} and $a_{-\max}$ are small, the tracking accuracy is high, but the system is one with slow response when the target's motion changes tremendously. If the absolute values of a_{\max} and $a_{-\max}$ are large, the system is one with quick response and lower tracking accuracy.

To avoid the negative influence of the limited acceleration presupposed in the target tracking, the functional relation between the maneuvering status of target and the estimation of the neighboring position information is used to carry out the adaptation of the process noise covariance.

Take the case of x , since the predicted quantity $\hat{x}(k|k-1)$ does not take account of the acceleration increment Δa_x , which the estimate $\hat{x}(k|k)$ contains, Δa_x can be approximated [13] by the deviation relationship between $\hat{x}(k|k-1)$ and $\hat{x}(k|k)$ using

$$\hat{x}(k|k) - \hat{x}(k|k-1) = \frac{T^2}{2} \Delta a_x \quad (25)$$

where T is the sampling interval.

Seen from (7), the variance of the maneuvering acceleration σ_a^2 is linear with the acceleration increment, while the acceleration increment Δa_x varies linearly with the position increment as shown in (25). Based on the above discussion, a developed adaptive Kalman algorithm [13], [14] is introduced Let

$$\sigma_a^2 = \lambda \times \frac{2}{T^2} |\hat{x}(k|k) - \hat{x}(k|k-1)| \quad (26)$$

where λ is a scale factor. Then the process noise covariance matrix can be rewritten as (27),

$$Q(k) = 2\alpha\sigma_a^2 \begin{pmatrix} q_{11} & q_{12} & q_{13} \\ q_{12} & q_{22} & q_{23} \\ q_{13} & q_{23} & q_{33} \end{pmatrix} = \lambda \times \frac{4\alpha}{T^2} \times |\hat{x}(k|k) - \hat{x}(k|k-1)| \times \begin{pmatrix} q_{11} & q_{12} & q_{13} \\ q_{12} & q_{22} & q_{23} \\ q_{13} & q_{23} & q_{33} \end{pmatrix} \quad (27)$$

According to (27), when the target is in low-speed maneuvering or non-maneuvering condition, the value of maneuvering acceleration variance σ_a^2 is small since there is little difference between $\hat{x}(k|k)$ and $\hat{x}(k|k-1)$. On the contrary, the value of maneuvering acceleration variance σ_a^2 gets larger along with the difference between $\hat{x}(k|k)$ and $\hat{x}(k|k-1)$ if the target is in high-

speed maneuvering condition. The equation (27) can reflect the state of maneuvering target correctly, which does not use a_{\max} and $a_{-\max}$.

As shown in (27), the process noise covariance matrix $Q(k)$ only contains the latest information of the motion. If the target's motion changed, the old data cannot reflect the current motion. However, if the target is in low-speed maneuvering or non-maneuvering condition, the UKF, which can obtain little information of the old data, is relatively sensitive and easily disturbed by noises. Hence the way of modified Sage-Husa [10] is introduced, which reduces the influence of the old data slowly.

Assume $Q(k)$ are unknown, then the corresponding Sage-Husa process noise statistics estimator [15] is given by

$$q(k) = \frac{1}{k} \sum_{j=1}^k [X(j|k) - \Phi(j-1)X(j-1|k)] \quad (28)$$

$$Q(k) = \frac{1}{k} \sum_{j=1}^k ([X(j|k) - \Phi(j-1)X(j-1|k) - q(k)] \times [X(j|k) - \Phi(j-1)X(j-1|k) - q(k)]^T) \quad (29)$$

In maneuvering target tracking, the effect of the latest information should be emphasized much more. The recursive modified Sage-Husa estimator [10] can be obtained as shown in (30),

$$Q(k) = (1 - d_{k-1})Q(k-1) + d_{k-1}[K(k)V(k)V^T(k)K^T(k) + P(k|k) - \Phi(k)P(k-1|k-1)\Phi^T(k)] \quad (30)$$

where $Q(k-1)$ is the process noise covariance matrix at timestep $k-1$ and d_{k-1} is the weighting coefficient of $Q(k-1)$. For simplicity, let

$$\hat{Q}(k) = K(k)V(k)V^T(k)K^T(k) + P(k|k) - \Phi(k)P(k-1|k-1)\Phi^T(k) \quad (31)$$

where $\hat{Q}(k)$ is the information of the process noise covariance matrix at timestep k .

By using the exponentially weighted fading memory method [13], weighting coefficient d can be chosen using

$$d_j = d_{j-1}b^j, \quad 0 < b < 1, \quad \sum_{j=0}^{k-1} d_j = 1 \quad (32)$$

where b is a forgetting factor, the initial value of d is set as 0.98 in the simulation and experiment. Then the following equation can be gotten.

$$d_{k-1} = (1-b)/(1-b^k) \quad (33)$$

Equation (27) is the process noise covariance matrix at timestep k for current statistical model based UKF and used to replace $\hat{Q}(k)$ here. Then a recursive modified process noise covariance matrix can be obtained as shown in (34),

$$Q(k) = (1 - d_{k-1})Q(k-1) + d_{k-1} \times \lambda \times \frac{4\alpha}{T^2} \times$$

$$|\hat{x}(k|k) - \hat{x}(k|k-1)| \times \begin{pmatrix} q_{11} & q_{12} & q_{13} \\ q_{12} & q_{22} & q_{23} \\ q_{13} & q_{23} & q_{33} \end{pmatrix} \quad (34)$$

B. Adaptive Algorithm of Measurement Noise Covariance Matrix $R(k)$

In this section, a fuzzy adaptive UKF is applied to estimate measurement noise covariance matrix $R(k)$. Fuzzy controller is one of the useful control paradigms for uncertain and ill-defined nonlinear systems. Control actions of a fuzzy controller are described by some linguistic rules. $R(k)$ is adjusted by monitoring the innovation sequence $\{\varepsilon(i), i=1, \dots, k\}$, which [16] is defined by

$$\varepsilon(i) = RSSI(i) - RSSI(i|i-1) \quad (35)$$

where $RSSI(i)$ is the real measurement and $RSSI(i|i-1)$ is the predicted value of $RSSI(i)$. The innovation sequence represents the information in the new observation and is considered as the most relevant source of information for the filter adaptation. In theory, innovation sequence is zero mean white Gaussian noise sequence as shown in (36),

$$E[\varepsilon(i)] = 0 \quad (36)$$

And the theoretical covariance matrix of $\varepsilon(i)$ can be derived from the UKF using

$$P_{zz} = \sum_{i=0}^{2N} W_i^{(m)} ([RSSI_i^*(k|k-1) - RSSI(k|k-1)] \times [RSSI_i^*(k|k-1) - RSSI(k|k-1)]^T) + R(k) \quad (37)$$

However, in practice, the innovation sequence is bothered by model uncertainty and noise statistical uncertainty. The method in [17] is used to obtain the mean and covariance matrix of the innovation sequence as shown in (38),

$$E'[\varepsilon(k)] = \frac{1}{N} \sum_{i=k-N+1}^k \varepsilon(i) \quad (38)$$

$$P'[\varepsilon(k)] = \frac{1}{N} \sum_{i=k-N+1}^k \varepsilon(i)\varepsilon^T(i)$$

N is chosen empirically to give some statistical smoothing. Then the error formula between theoretical covariance matrix and practical covariance matrix of the innovation sequence are gotten by using

$$\Delta P'[\varepsilon(k)] = P'[\varepsilon(k)] - P_{zz} = \frac{1}{N} \sum_{i=k-N+1}^k \varepsilon(i)\varepsilon^T(i) - \sum_{i=0}^{2N} W_i^{(m)} ([RSSI_i^*(k|k-1) - RSSI(k|k-1)] \times [RSSI_i^*(k|k-1) - RSSI(k|k-1)]^T) - R(k) \quad (39)$$

It is noteworthy that $\Delta P'$, whose value should be zero in optimal situation, reflects the state of current Kalman

filter. When the values of E' and $\Delta P'$ are not zero, it indicates that the prediction of $RSSI(k)$ is not correct. Then $R(k)$ is adjusted to make the Kalman filter tend towards stability. The adjustment rules of $R(k)$ are as follows:

- (1) If $\Delta P' = 0$, $R(k)$ remains unchanged.
- (2) If $\Delta P' > 0$, $R(k)$ increases.
- (3) If $\Delta P' < 0$, $R(k)$ decreases.

Based on the adjustment rules above, $\Delta P'$ are chosen as the input variables of fuzzy logical controller. The fuzzy method proposed here receives the value of $\Delta P'$ every timestep and works out a scale parameter called the adjustment factor β . The β indicates the amount which the measurement noise covariance matrix $R(k)$ should be scaled by, in order to compensate for the varying noise disturbances. The measurement noise covariance [15] at timestep k is calculated using,

$$\hat{R}(k) = \beta R(k) \quad (40)$$

The range of β is [0.0001, 2] and its initial value is set as 1 in the simulation and experiment, while the range of $\Delta P'$ is set as [-0.1, 0.1].

The input linguistic variable is $\Delta P'$ and the input linguistic values are N : Negative, ZE : Zero and P : Positive, while triangular membership function is used in the input space. Correspondingly, β is the output linguistic variable and the output linguistic values are PS : Positive Small, PM : Positive Medium, and PB : Positive Big, while trapezoidal membership function is used. Fig. 1 shows the membership functions of input and output variables.

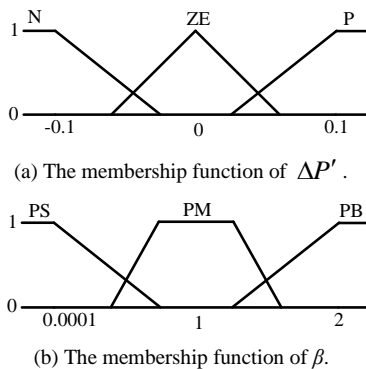


Fig. 1. The membership functions of input and output variables.

IV. SIMULATION

In order to verify the feasibility and efficiency of the proposed algorithm in this paper, the CAUKF, AUKF in [10] and the final improved CAUKF are simulated. Simulation with the same parameters is implemented on the MATLAB R2010a software.

The coordinates of four reference nodes are (0,0,0), (0,100m,0), (100m,0,0) and (0,0,100m) respectively. Three kinds of tracking task are simulated. The first task

is tracking a target travelling in uniform rectilinear motion with a velocity of 2m/s in x-direction, y-direction and z-direction. The second task is tracking a motion whose acceleration changes sharply during the movement. In the beginning the velocities of x-direction and y-direction are both 20m/s, while the accelerations are both 1m/s². After 14 seconds, the accelerations of x-direction and y-direction change to 30m/s². The velocity of z-direction remains 1m/s during the entire time. The zigzag-line motion tracking is the third task. The velocities of x-direction and z-direction are 1m/s and the y-direction velocity is 10m/s, which changes to -10m/s after 9 seconds.

The sampling interval T is 0.28s. The initial value of the state estimate is

$$X(k) = [0 \ 0 \ 0 \ 0 \ 0 \ 0 \ 0 \ 0 \ 0] \quad (41)$$

while the initial value of covariance matrix is

$$P(0) = \text{diag}\{0.1, 0.1, 0.1, 0.1, 0.1, 0.1, 0.1, 0.1, 0.1\} \quad (42)$$

Q and R are designed to change as

$$Q(t) = \begin{cases} \text{diag}\{0.001^2, 0, 0, 0.001^2, 0, 0, 0.001^2, 0, 0\}, & 0 \leq t < 8.4 \\ \text{diag}\{0.003^2, 0, 0, 0.003^2, 0, 0, 0.003^2, 0, 0\}, & 8.4 \leq t < 16.8 \\ \text{diag}\{0.002^2, 0, 0, 0.002^2, 0, 0, 0.002^2, 0, 0\}, & 16.8 \leq t < 28 \end{cases} \quad (43)$$

$$R = \text{diag}\{0.001^2, 0.001^2, 0.001^2, 0.001^2\} \quad (44)$$

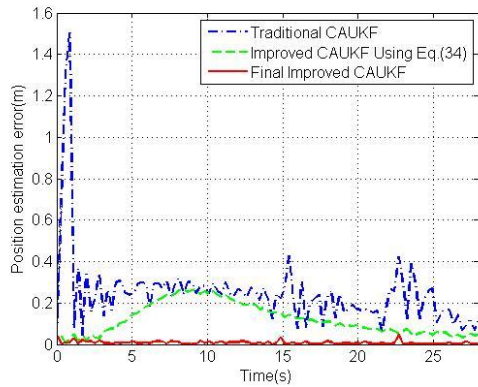
The position estimation error is used as a criterion to compare the different computation methods and defined by

$$\text{Error} = |\hat{x}(k) - x(k)| + |\hat{y}(k) - y(k)| + |\hat{z}(k) - z(k)| \quad (45)$$

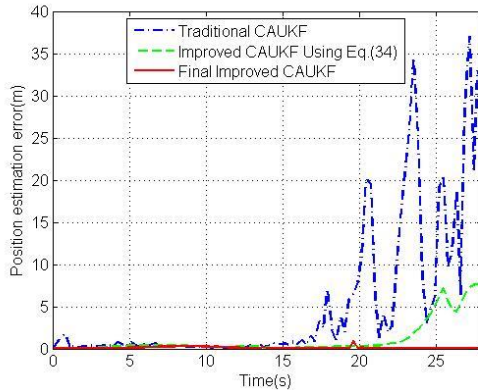
where $x(k)$, $y(k)$ and $z(k)$ are the real measurement values, while $\hat{x}(k)$, $\hat{y}(k)$ and $\hat{z}(k)$ are the predicted values respectively.

For comparison, the proposed algorithms are simulated firstly, which contain the traditional CAUKF with $Q(k)$ in (27), the improved CAUKF with adaptive algorithm of $Q(k)$ in (34) and the final improved CAUKF with both adaptive algorithm of $Q(k)$ in (34) and $R(k)$ mentioned in 3.2. The results are shown in Fig. 2.

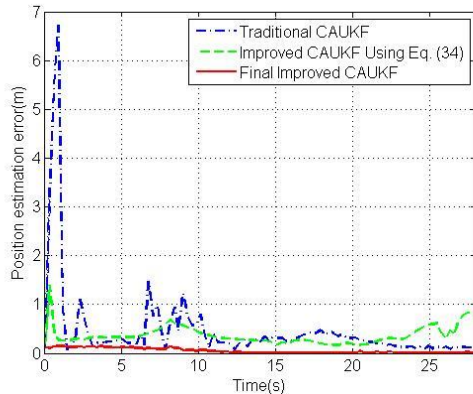
As shown in Fig. 2, the final improved CAUKF performs much better than traditional CAUKF and improved CAUKF with $Q(k)$ in (34). Since the process noise $Q(k)$ in (27) only contains the latest information of the motion, the estimation error is easily disturbed, which fluctuates unsteadily, especially when the target highly maneuvers. The estimation errors of the improved CAUKF with $Q(k)$ in (34) and final improved CAUKF with both adaptive algorithm of $Q(k)$ and $R(k)$ follow a relatively smooth curves as shown in Fig. 2. However, the accuracy of final improved CAUKF is the best of all the three methods. Also, Fig. 2 shows the faster convergence speed of the proposed algorithm.



(a) Track a target in uniform rectilinear motion.



(b) Track a motion whose acceleration changes sharply during the movement.



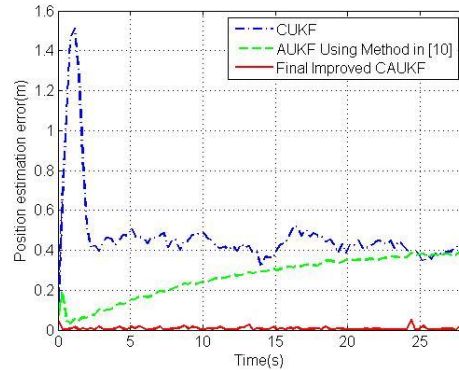
(c) Track zigzag-line motion

Fig. 2. The simulation results of Traditional CAUKF, Improved CAUKF with $Q(k)$ in (34) and final Improved CAUKF.

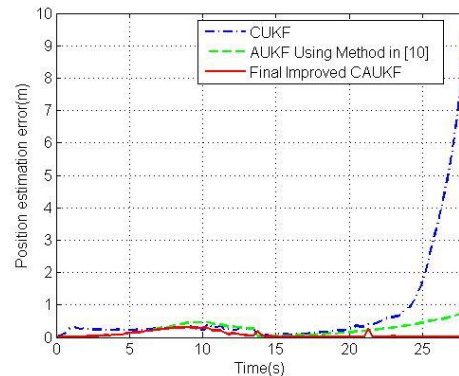
Then the CUKF, AUKF using the method in [10] and our final improved CAUKF are compared with each other. The results of the simulation are shown in Fig. 3.

In Fig. 3(a), the results show that our final improved CAUKF features faster response and smaller overshoot if the target is in uniform rectilinear motion. This effect can be observed more clearly in Fig. 3(b) and Fig. 3(c). If the target changes its motion mode, CUKF is much easier to be affected than AUKF using method in [10] and the final improved CAUKF, which gets larger overshoot and slower convergence speed. Since the unknown process noise can lead to large estimation errors, the state estimate of standard UKF sometimes may deviate from

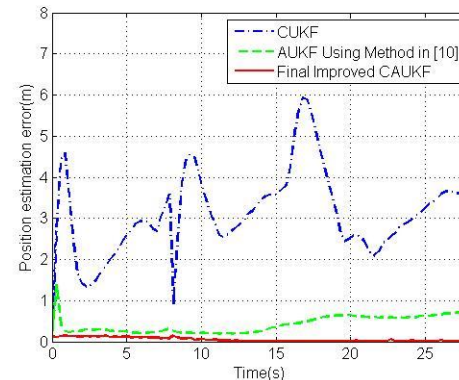
the true state a lot, especially when the target is in high-speed maneuvering condition. The performance of AUKF using the method in [10] is much better than that of standard UKF. However, Fig. 3 shows that the final improved CAUKF can change along with the maneuvering target more quickly and track the target's sharp movement change more accurately. Also, it can be seen obviously that the final improved CAUKF can get better estimation accuracy than AUKF using the method in [10].



(a) Track a target in uniform rectilinear motion.



(b) Track a motion whose acceleration changes sharply during the movement.



(c) Track zigzag-line motion

Fig. 3. The simulation results of CUKF, AUKF using method in [10] and our final Improved CAUKF.

V. EXPERIMENTAL RESULTS

Experiments were carried out in an indoor environment to test and validate the proposed algorithm mentioned in

previous sections. Error caused by reflection due to the antenna diversity can be reduced by setting the antenna of each reference node at the angle of 90 degrees at the mounting surface. Six nodes are used in the experiments. One node is designated as the target, which broadcasts to any reference node that is listening. In order to track the real-time position of the moving target node, four reference nodes are placed in indoor environment. Cartesian coordinates are established in indoor environment, where x-y plane is the ground. Three of the reference nodes are placed on the x-y plane, which are (0, 0) (0,10m) (10m, 0), while the other one is placed 1m above the node (0, 0). The last node is connected to a personal computer that collects RSSI data of the reference nodes and performs tracking algorithms. The nodes are designed based on C2430, which is 2.4GHz IEEE 802.15.4 compliant RF transceiver developed by TI. In order to drown out disturbing noise, the RSSI value between target node and each reference node is measured 10 times every timestep and the average is regarded as the final measurement value.

In this experiment, two kinds of tracking tasks are tested. The first task is tracking a manipulator travelling in uniform rectilinear motion with a velocity of 1m/s. The second task is tracking a manipulator travelling in uniform circular motion with a radius of 10m and an angular velocity of 0.15rad/s.

As in the simulation, the position estimation error comparison of traditional CAUKF with $Q(k)$ in (27), improved CAUKF with $Q(k)$ in (34), and final improved CAUKF with both adaptive algorithms in section III is analyzed, which is shown in Fig. 4. And Fig. 5 shows the results based on the CUKF, AUKF using the method in [10] and our final improved CAUKF, respectively.

The average root mean square error (RMSE) can be used to evaluate the performances of the algorithms as shown in (46),

$$E(RMSE) = \frac{1}{k} \sum_{i=1}^k \sqrt{\frac{1}{N} \sum_{j=1}^N [(\hat{x}(i) - x(j))^2 + (\hat{y}(i) - y(j))^2 + (\hat{z}(i) - z(j))^2]} \quad (46)$$

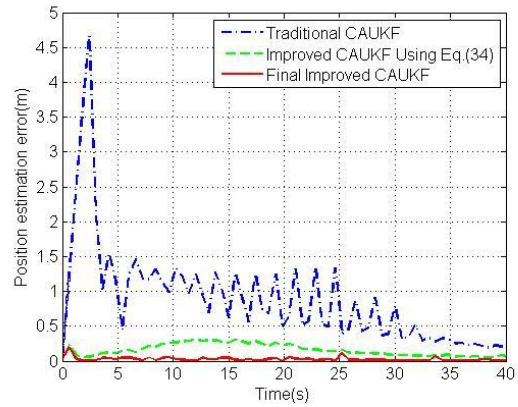
where N is the measurement times every timestep, which is 10 in the experiment. k is the iteration times.

The average RMSE of each algorithm is shown in Table I.

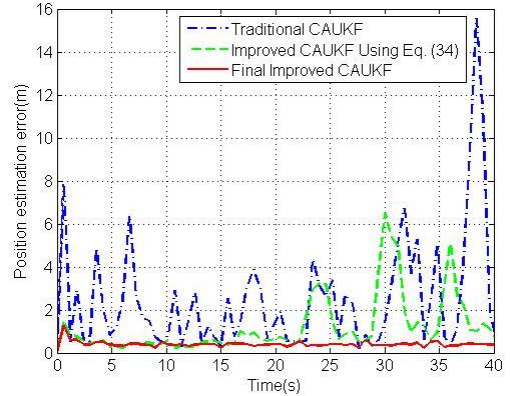
	CUKF	AUKF using method in [10]	Final improved CAUKF
Average RMSE of uniform rectilinear motion	0.7923	0.5723	0.1071
Average RMSE of uniform circular motion	1.0963	0.7219	0.1968

Fig. 4 and Fig. 5 show that our final improved CAUKF features faster response and smaller overshoot if the target is in uniform rectilinear motion. The final

estimation error of final improved CAUKF is smaller than those of the other algorithms. As shown in Fig. 5(b), when the target is in uniform circular motion, the estimation error of the final improved CAUKF reaches a small value quickly in the first 2 seconds and the final estimation error remains below 1m. However, the estimation error of the AUKF using the method in [10] remains a large value and the final estimation error is between 2m and 3m. Seen from Table I, the average RMSE of final improved CAUKF position estimations is obviously less than those of the other algorithms. Generally, the experimental results show that the proposed algorithm has better performance.

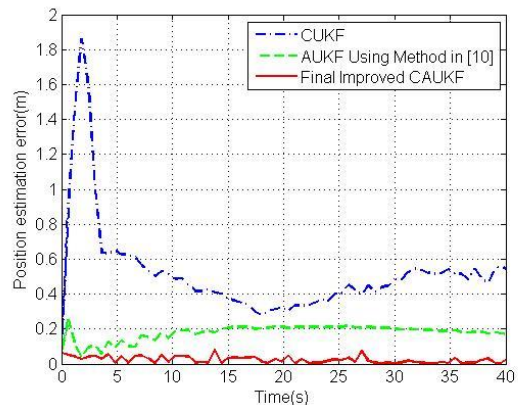


(a) Track a manipulator in uniform rectilinear motion.

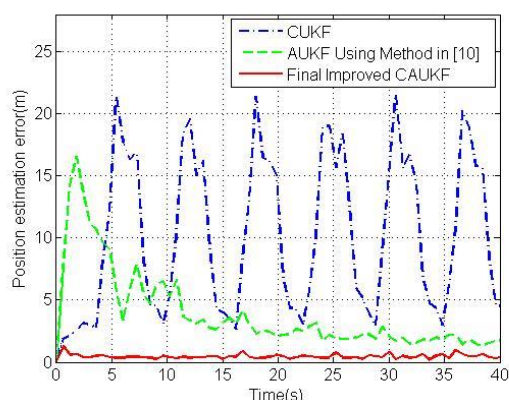


(b) Track a manipulator in uniform circular motion.

Fig. 4. Experimental results of CAUKF, Improved CAUKF with $Q(k)$ in (34) and final Improved CAUKF.



(a) Track a manipulator in uniform rectilinear motion.



(b) Track a manipulator in uniform circular motion.

Fig. 5. Experimental results of CUKF, AUKF using method in [10] and our final Improved CAUKF.

VI. CONCLUSIONS

In this paper, an improved CAUKF for wireless sensor network is proposed to track a maneuvering target. This method can not only track a target in low-speed maneuvering or non-maneuvering condition, but also a target in high-speed maneuvering condition. In order to introduce the improved adaptive UKF algorithm, a current statistical model based on RSSI is built, which can describe the trajectory of a maneuvering target. Based on the current statistical model, a developed adaptive UKF algorithm is proposed, which estimates the process noise covariance matrix $Q(k)$ by the way of modified Sage-Husa estimator. Then an improved fuzzy adaptive UKF is used to estimate the covariance matrices $R(k)$. The simulation and experimental results show that the final improved CAUKF can reduce the estimation error and sense the variation of the motion faster.

REFERENCES

- [1] Y. B. Yao, Q. Han, X. R. Xu, and N. L. Jiang, "A RSSI-Based distributed weighted search localization algorithm for WSNs," *International Journal of Distributed Sensor Networks*, vol. 2015, pp. 1-11, 2015.
- [2] Q. D. Dong and X. Xu, "A novel weighted centroid localization algorithm based on RSSI for an outdoor environment," *Journal of Communications*, vol. 9, no. 3, pp. 279-285, 2014.
- [3] H. Liu, H. S. Darabi, P. Banerjee, and J. Liu, "Survey of wireless indoor positioning techniques and systems," *IEEE Transactions on Systems, Man, and Cybernetics-Part C: Applications and Reviews*, vol. 37, no. 6, pp. 1067-1080, 2007.
- [4] Y. F. Zhao, H. Ren, and J. F. Hu, "A simultaneous localization and tracking algorithm based on compressing kalman filter," *Sensors & Transducers*, vol. 177, no. 8, pp. 1-6, 2014.
- [5] S. Y. Chen, "Kalman filter for robot vision: A survey," *IEEE Transactions on Industrial Electronics*, vol. 59, no. 11, pp. 4409-4420, 2011.
- [6] F. Gustafsson and G. Hendeby, "Some relations between extended and unscented kalman filters," *IEEE Transactions on Signal Processing*, vol. 60, no. 2, pp. 545-555, 2011.
- [7] S. Jafarzadeh, C. Lascu, and M. S. Fadali, "State estimation of induction motor drives using the unscented Kalman filter," *IEEE Transactions on Industrial Electronics*, vol. 59, no. 11, pp. 4207-4216, 2011.
- [8] H. R. Zhou and K. S. P. Kumar, "A 'current' statistical model and adaptive algorithm for estimating maneuvering targets," *Journal of Guidance Control & Dynamics*, vol. 7, no. 5, pp. 596-602, 1984.
- [9] J. Wei, C. C. Liu, W. L. Guo, and Y. Z. Cai, "Improved current statistical model algorithm for maneuvering target tracking," *Aerospace Shanghai*, vol. 31, no. 2, pp. 52-56, 2014.
- [10] Y. Shi and C. Z. Han, "Adaptive UKF method with applications to target tracking," *Acta Automatica Sinica*, vol. 37, no. 6, pp. 755-759, 2011.
- [11] Q. F. He, Y. B. Li, H. Lv, and G. J. He, "Switching multisensor improved current statistical model for maneuvering target tracking," *Applied Mechanics and Materials*, vol. 385-386, pp. 585-588, 2013.
- [12] P. M. Santos, T. E. Abrudan, A. Aguiar, and J. Barros, "Impact of position errors on path loss model estimation for device-to-device channels," *IEEE Transactions on Wireless Communications*, vol. 13, no. 5, pp. 2353-2361, 2014.
- [13] J. Dunik, M. Simandl, and O. Straka, "Unscented Kalman filter: Aspects and adaptive setting of scaling parameter," *IEEE Transactions on Automatic Control*, vol. 57, no. 9, pp. 2411-2416, 2012.
- [14] C. Liu, X. H. Huang, and M. Wang, "Target tracking for visual servoing systems based on an adaptive Kalman filter," *International Journal of Advanced Robotic Systems*, vol. 9, no. 149, pp. 1-12, 2012.
- [15] J. H. Cheng, D. D. Chen, R. J. Landry, L. Zhao, and D. X. Guan, "An adaptive unscented Kalman filtering algorithm for MEMS/GPS integrated navigation systems," *Journal of Applied Mathematics*, vol. 2014, pp. 1-8, 2014.
- [16] J. P. Li, X. X. Zhong, and I. T. Lu, "Three-dimensional node localization algorithm for WSN based on differential RSS irregular transmission model," *Journal of Communications*, vol. 9, no. 5, pp. 391-397, 2014.
- [17] M. Das, S. Sadhu, and T. K. Ghoshal, "An adaptive sigma point filter for nonlinear filtering problems," *International Journal of Electrical, Electronics and Computer Engineering*, vol. 2, no. 2, pp. 13-19, 2013.



Xiaojun Peng was born in China in 1980. He received the B.S. degree from Zhengzhou University (ZZU), Zhengzhou, in 2002 and the M.S. degree from Wuhan University (WHU), Wuhan, in 2006, both in physical electronics. He is currently pursuing the Ph.D. degree with the School of Optical and Electronic Information, Huazhong University of Science and Technology (HUST). His research interests include wireless communication, measurement and control, signal and image processing, and circuit designing.



Kuntao Yang was born in China in 1946. He is a professor of the School of Optical and Electronic Information, Huazhong University of Science and Technology (HUST). His research interests include fiber-optic communications, fiber-optic sensing technology, optoelectronic measurement and control.



Chang Liu was born in China in 1984. He received the B.S. degree in Automation, Ph.D. degree in Control Theory and Control Engineering from Huazhong University of Science and Technology (HUST) in 2007 and 2012, respectively. His research interests include visual servoing control, pattern recognition and image processing.